Contribution from the Departments of Chemistry, University of New Mexico, Albuquerque, New Mexico 87131, and Cornell University, Ithaca, New York 14853

Hydride Bridges between $LnCp_2$ Centers

J. V. ORTIZ*† and ROALD HOFFMANN‡

Received September 12, 1984

d orbitals of d^0f^x $LnCp_2$ fragments stabilize bridging hydrides in a variety of geometries. $SmCp_2$ a_1 orbitals are markedly different from MCp_2 a_1 orbitals, where M is an early transition metal of the fourth or fifth period. Symmetric hydride bridges are more stable than asymmetric ones. Various deployments of symmetric bridges use different $LnCp_2$ orbitals. When the Cp–Ln–Cp planes coincide in $(Cp_2LnH)_2$, the Ln_2H_2 plane is perpendicular to the Cp_2Ln planes. When the Cp_2Ln planes are orthogonal, the Ln_2H_2 plane bisects them. Possible placements of terminal hydrides are determined by the $2a_1$ orbital of the $SmCp_2$ fragment. Bonding in complexes of the type $(LnCp_2X)_3X^-$ (X = H, Cl) is discussed.

Discrete organolanthanide hydride molecules have recently been synthesized. The hydrides form bridges between two or three metal atoms, but the symmetry of their deployment is uncertain. Precedents from main-group and transition-element electron-deficient structures include symmetric (**1a**) and asymmetric (**1b**) bridges, and it is interesting to inquire about the symmetry or asymmetry of the lanthanide hydrides.

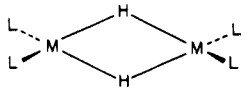

1a

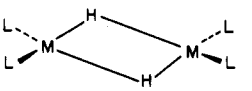

1b

An unusual arrangement of ligands has appeared in which the terminal L–M–L planes are nearly perpendicular[1] (**2**). The

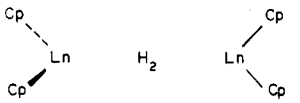

2

positions of the hydrogen bridges are unknown. Counting the Cp rings as anions and the bridging ligands as hydrides gives Ln^{3+}. For the lanthanides, this implies an atomic configuration of $5d^06s^06p^04f^x$.

Compounds of the formula $(Cp_2(THF)M(\mu\text{-}H))_2$, where M = Y, Er, Lu, also have structures with bridging hydrides and oxygen ligands that lie within or close to the M_2H_2 plane[2] (**3**). The

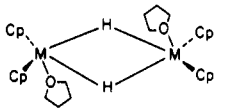

3

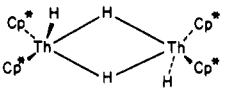

4

oxidation state remains 3+. Related structures with Zr instead of lanthanides replace the oxygen ligands with more hydrides,[3] moving to a Zr^{4+} oxidation state for two more hydrides. Similar compounds are obtained in the actinide series. Thus, Marks and co-workers, working with Th complexes, observe the placement of terminal hydrides above and below the M_2H_2 plane in $(Cp^*_2ThH(\mu\text{-}H))_2$[4] (**4**). A trinuclear system, $(Cp_2ErH)_3Cl^-$ (**5**), has also emerged from these studies. Two distinct types of bridging, between two or three centers, are observed in this Er(III) complex.[5] The lanthanide hydrides are a fascinating group of compounds. The geometrical preferences of the dinuclear and trinuclear hydrides in this series are the subject of our work.

The Cp_2Sm Fragment and Its Relationship to Corresponding Transition-Metal Fragments

The lanthanide hydride complexes that we have mentioned all contain a d^0 Cp_2Ln^+ fragment, which then forms a natural starting

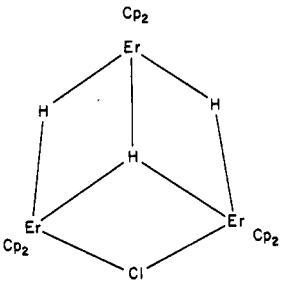

5

point for our theoretical discussion. Let us examine the orbitals of the Cp_2Sm^+ fragment as a function of the angle Cp(centroid)–M–Cp(centroid), ϕ, defined, along with the coordinate system we will use throughout this work, in **6**. Placing the Sm

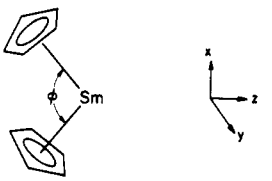

6

atom at the origin of the coordinate system, we see that at ϕ = 180° the line connecting the metal atom to the Cp centroids will overlap with the x axis. As ϕ is made smaller, the Cp centroids are located in the xz plane at points with neg. z values.

Valence energy levels of the $SmCp_2^+$ fragment as a function of the Cp(centroid)–M–Cp(centroid) angle are displayed in Figure 1. The f-orbital levels at the bottom are only slightly perturbed by the ligand environment, the largest destabilization with respect to the atomic f orbital H_{ii} being approximately 0.1 eV. Hybridizations with the s, p, and d orbitals of Sm are therefore very small. The remaining levels are all unoccupied. Combinations of Cp $\pi^*(e_2)$ levels lie between the Sm d and f orbitals. These interact little with further ligands and will not concern us further.

At the D_{5h} sandwich geometry (ϕ = 180°) the orbitals split into a typical pattern, $a_{1g} < e_{2g} < e_{1g}$. There is a tricky problem with the coordinate systems here. The natural choice for the z axis

† University of New Mexico.
‡ Cornell University.

(1) Evans, W. J.; Bloom, I.; Hunter, W. E.; Atwood, J. L. *J. Am. Chem. Soc.* **1983**, *105*, 1401–3.
(2) Evans, W. J.; Meadows, J. H.; Wayda, A. L.; Hunter, W. E.; Atwood, J. L. *J. Am. Chem. Soc.* **1982**, *104*, 2008–14.
(3) Jones, S. B.; Petersen, J. L. *Inorg. Chem.* **1981**, *20*, 2889–94.
(4) Broach, R. W.; Schultz, A. J.; Williams, J. M.; Brown, G. M.; Manriquez, J. M.; Fagan, P. J.; Marks, T. J. *Science (Washington, D.C.)* **1979**, *203*, 172–4. Fagan, P. J.; Manriquez, J. M.; Maata, E. A.; Seyam, A. M.; Marks, T. J. *J. Am. Chem. Soc.* **1981**, *103*, 6650–67. Manriquez, J. M.; Fagan, P. J.; Marks, T. J. *J. Am. Chem. Soc.* **1978**, *100*, 3939–41.
(5) Evans, W. J.; Meadows, J. H.; Wayda, A. L. *J. Am. Chem. Soc.* **1982**, *104*, 2015–7.

0020-1669/85/1324-2095$01.50/0

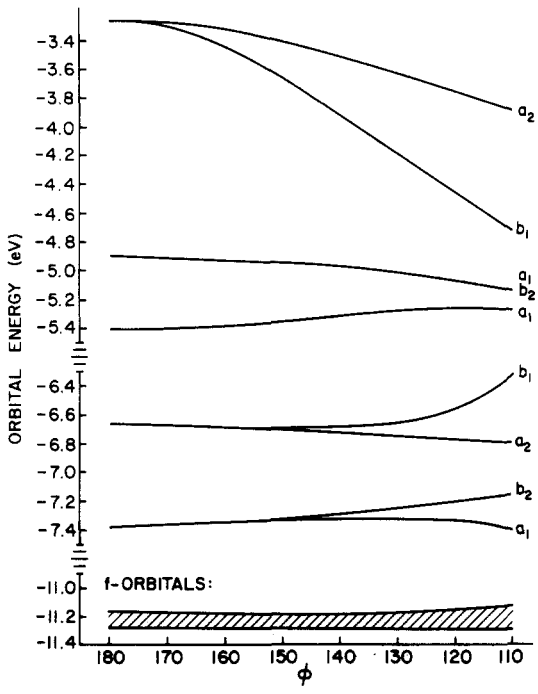

Figure 1.

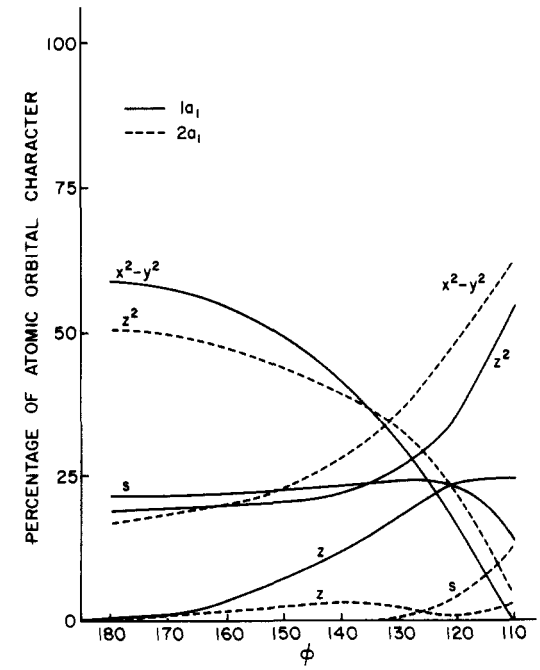

Figure 2.

in the D_{5h} structure would be the fivefold axis. But the moment ϕ decreases from 180°, and the symmetry is lowered to C_{2v}, the C_2 axis orthogonal to the original fivefold axis is the canonical choice for the z axis. We have taken consistently that latter axis system, as **6** shows. Thus the fivefold axis is x and the orbitals that we would have called z^2 (a_{1g}), $x^2 - y^2$, xy (e_{2g}), and xz, yz (e_{1g}) had we had z as the fivefold axis now become x^2 (a_{1g}), $y^2 - z^2$, yz (e_{2g}), and xy, xz (e_{1g}). As ϕ is varied, the degeneracies are removed. The two highest d levels, labeled a_2 and b_1, are predominantly xy and xz Sm orbitals. Their composition changes very little with ϕ. Below these are the nearly degenerate set of a_1 and b_2 orbitals that correlate with yz and $y^2 - z^2$ orbitals in the $\phi = 180°$ case. Finally, there is the lowest a_1 d orbital, which correlates with x^2 in the $\phi = 180°$ case. As ϕ decreases, the lowest orbital is gradually transformed, at small ϕ, into a mix of s, z, and z^2 that points away from the two Cp rings. The second a_1 d orbital becomes mostly $x^2 - y^2$ in character, but only for small

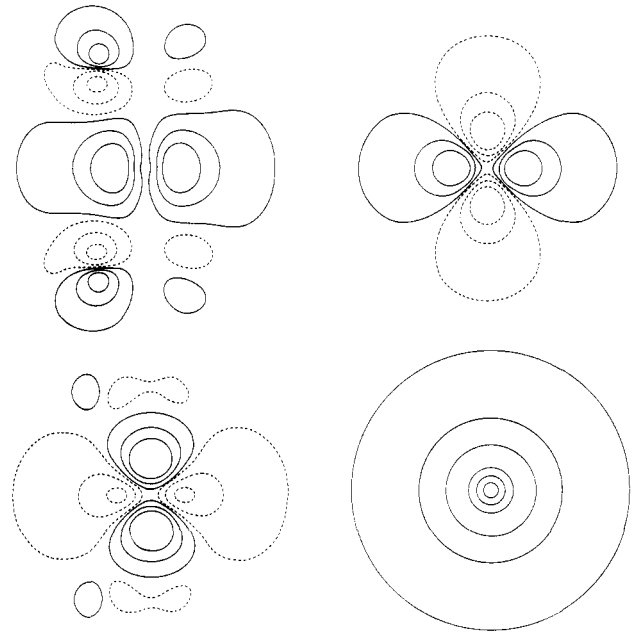

Figure 3. $SmCp_2$ orbital plots: (bottom row) $1a_1$; (top row) $2a_1$; (left column) xz plane; (right column) yz plane.

ϕ. Figure 2 shows the changes in atomic orbital character for the a_1 orbitals. The b_2 orbital remains chiefly a yz orbital throughout.

At $\phi = 130°$, some orbital plots were made. Figure 3 gives the xz and yz plots of the lowest a_1 d orbital. The x^2 character is clearly dominant. The same cross sections for the next highest $2a_1$ level are also shown in the figure. A $z^2 - y^2$ orbital is depicted.

We now see the primary difference between the orbitals of Cp_2Ti, a typical transition-metal analogue, and the lanthanide. In reference to our earlier work,[6] in Cp_2Ti the $1a_1$ level approximates a y^2 orbital and $2a_1$ is a hybrid of s, z, and z^2. There is a tendency in that direction in the Cp_2Sm case, but the character of the a_1 levels is reversed and, more importantly, the hybridization is not so well developed. In a comparison of Cp_2Ti and Cp_2Sm at the same ϕ, the Cp_2Sm levels are much more like those at $\phi = 180°$ than the transition-metal levels. Later in the paper we will consider the changes in the nature of the orbitals as one moves across the lanthanide series.

The orbital diagrams are informative, but not very portable. If we need small symbols to inform us of the primary orbital character of the frontier orbitals, we would suggest those in **7**.

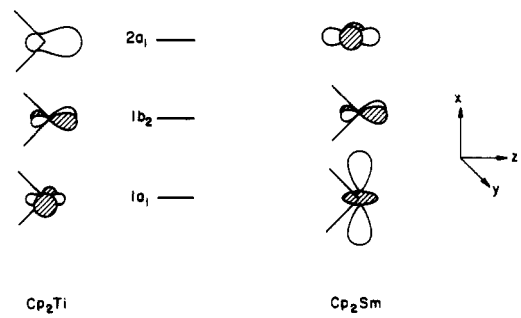

7

The energy differences between the d orbitals are much smaller than in the case of $TiCp_2$.[6] With the avoided crossing of the two levels of a_1 symmetry, three orbitals are within a few tenths of an electron volt. This will facilitate mixings of the fragment orbitals in the formation of σ bonds in the yz plane. Another important result is the rapid stabilization of the b_1 level as ϕ

(6) Lauher, J. W.; Hoffmann, R. *J. Am. Chem. Soc.* **1976**, *98*, 1729–42.

decreases. Donors approaching the *xz* plane might employ this acceptor orbital.

Calculations on the Cp_2Sm molecule predict an ordinary sandwich arrangement, $\phi = 180°$, to be most stable. Distortions of the Cp–Sm–Cp angle are not energetically costly, however. Reducing the angle from 180 to 130° requires only 0.06 eV, as none of the d levels are filled and the f orbitals are insensitive to environmental changes. Collapse of this angle below 120° is chiefly prevented by repulsions between the π levels of the individual Cp units. Recently $(C_5Me_5)_2Sm$ has been synthesized and its structure determined.[7] The ring centroid–Sm–ring centroid angle in this remarkable monomeric compound is 140.1°.

We are now ready to form some of the Cp_2Ln hydrides.

Cp_2SmH and $(Cp_2SmH)_2$

It is useful to begin by analyzing the preferred disposition of a single hydride relative to a single Cp_2Sm unit. Consider the hypothetical Cp_2SmH (**8a**), where H lies in the *yz* plane but not

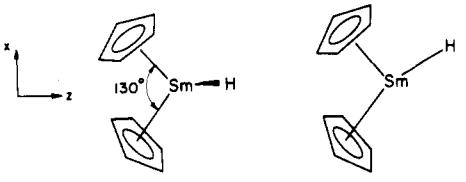

8a **8b**

along the *z* axis. Good H^- to Cp_2Sm^+ overlap populations from 1s to $1a_1$ and 1s to $1b_2$ stabilize the hydride. In the latter case, one of the lobes of *yz* interacts with the 1s orbital as in **9a**. In

9a **9b**

the former case, the 1s orbital sees the central, circular lobe of the x^2 orbital (**9b**). Suppose the hydride is rotated into the *xz* plane, as in **8b**. The 1s to $1b_1$ interaction then becomes important, as shown in **10a**. The interaction with $1b_2$ vanishes as the hydride

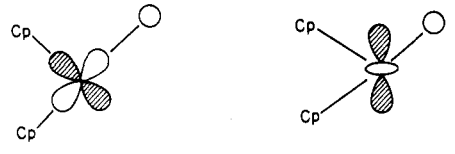

10a **10b**

is in a nodal plane of this orbital. The 1s to $1a_1$ interaction (**10b**) is diminished by this geometrical change since the hydride is starting to approach a nodal plane of $1a_1$.

The geometrical change described is **11** → **12**. For this transit

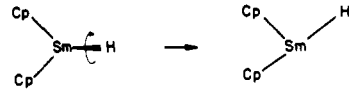

11 **12**

the overlap population of 1s with $1a_1$ will decline, with $1b_2$ will decrease and vanish, and with $1b_1$ will increase from zero. The net effect of $1b_1$ and $1b_2$ is very small, slightly favoring the final structure. The determining factor that causes the energy to rise for the transit is the fall of 1s to $1a_1$ overlap population.

(7) Evans, W. J.; Hughes, L. A.; Hanusa, T. P. *J. Am. Chem. Soc.* **1984**, *106*, 4270–2.

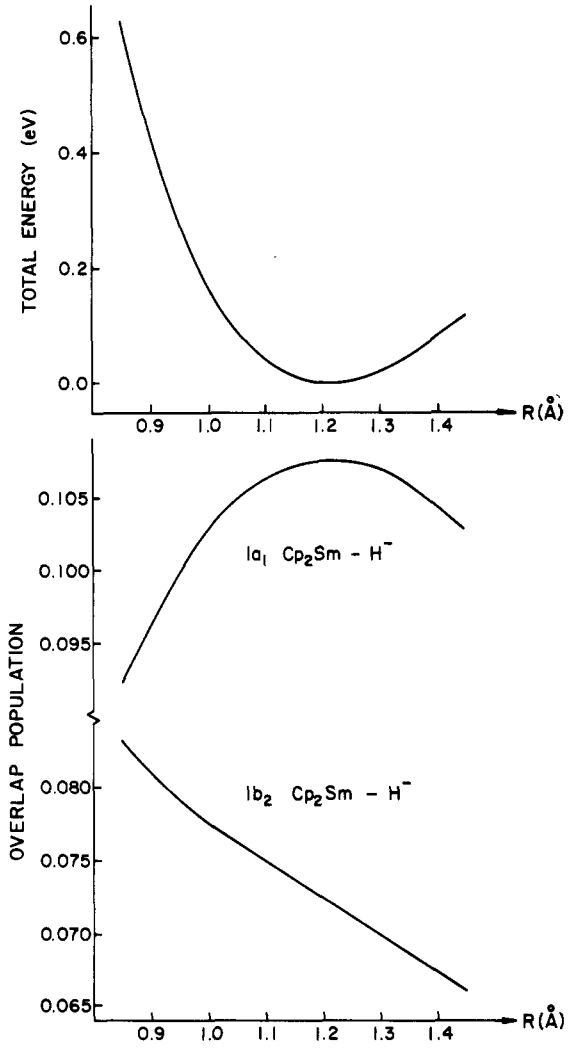

Figure 4.

Let us now consider the formation of a symmetrically bridged $(Cp_2SmH)_2$ dimer, in the geometry of **13**. One analysis of the

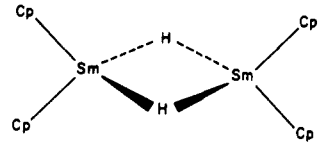

13

bonding might begin from 2 $(Cp_2Sm)^+$ and 2 H^-. The two hydride levels would form symmetric and antisymmetric combinations, and these in turn would be stabilized by mixing with the empty d orbitals of Cp_2Sm^+, primarily $1a_1$ and $1b_2$. The resultant orbitals are shown schematically in **14**.

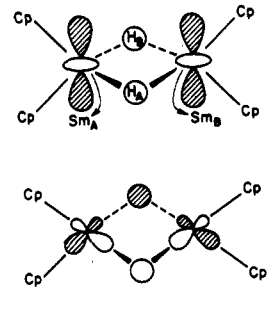

14

Calculations with $\phi = 130°$ and a Sm–Sm distance of 3.905 Å show the variation of total energy as the distance from the Sm–Sm midpoint for both hydrides, R, is changed (see Figure 4). The minimum, though shallow, reflects the competition of two dominant fragment overlap population curves, also shown in Figure 4. Largest of the hydride interactions is that with the $1a_1$ d orbital, and the minimum of the energy curve nearly coincides with the maximum of this fragment overlap population. The $2a_1$–hydride interaction is much smaller. $1b_2$ to hydride overlap populations are second in importance. They tend to shift the optimal Sm–H distance downward from the maximum suggested by the $1a_1$–hydride interaction alone.

As the extended Hückel method is often unreliable in determining bond lengths, the particular structure obtained here should not be taken too seriously. The observation of geometrical trends is the object of the study. As these trends depend on the variation of overlap and on the relative energies of the fragment orbitals, the location of a particular minimum is not of decisive importance.

With use of the optimized symmetric structure as a reference, distortions of the hydrogens within the Sm_2H_2 plane can be studied. For example, with fixed Sm_A–H_A and Sm_B–H_B distances, the angle θ describes a motion that destroys one of the reflection planes in the molecule but not the inversion center (**15**). In other

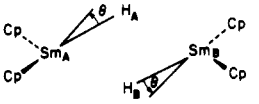

15

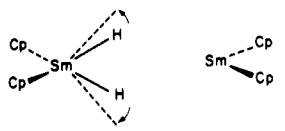

16

words, the hydrogen bridging is made asymmetrical. The computed energy rises as θ is increased from the symmetric bridging position. However, we do not necessarily trust these results because the extended Hückel method is not very good at dealing with the bond length changes that would accompany such a deformation. A deformation that would lead to $(Cp_2SmH_2)^-(Cp_2Sm)^+$ ion pairs (**16**) was also tested, and there was resistance to it.

Distortions that destroy the Sm_2H_2 plane are studied by variations in dihedral angles. In the reference structure, each Sm_2H plane forms a dihedral angle of 90° with the planes defined by the Sm atom and the centroids of the Cp ligands. This arrangement is symbolized by the diagram **17**, where the two solid

17 **18**

lines stand for the Cp(centroid)–Sm–Cp(centroid) planes and the two dotted lines stand for the Sm_2H planes. The variation of the angle α, defined in **18**, from 180° destroys the Sm_2H_2 plane but leaves the symmetric Sm–H–Sm bridges intact. H_A does not move from its original position; only H_B is affected by changing α.

Resistance to the reduction of α depends on two orbital energies (see Figure 5). The first crucial orbital has dominant contributions from the two hydride orbitals in symmetric combination (**19a**). This orbital mixes with Cp_2Sm^+ orbitals of the a_1 type.

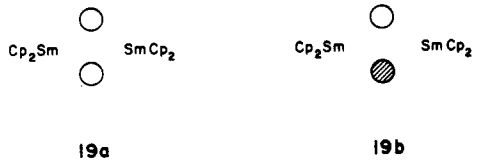

19a **19b**

The higher lying antisymmetric combination (**19b**) mixes with

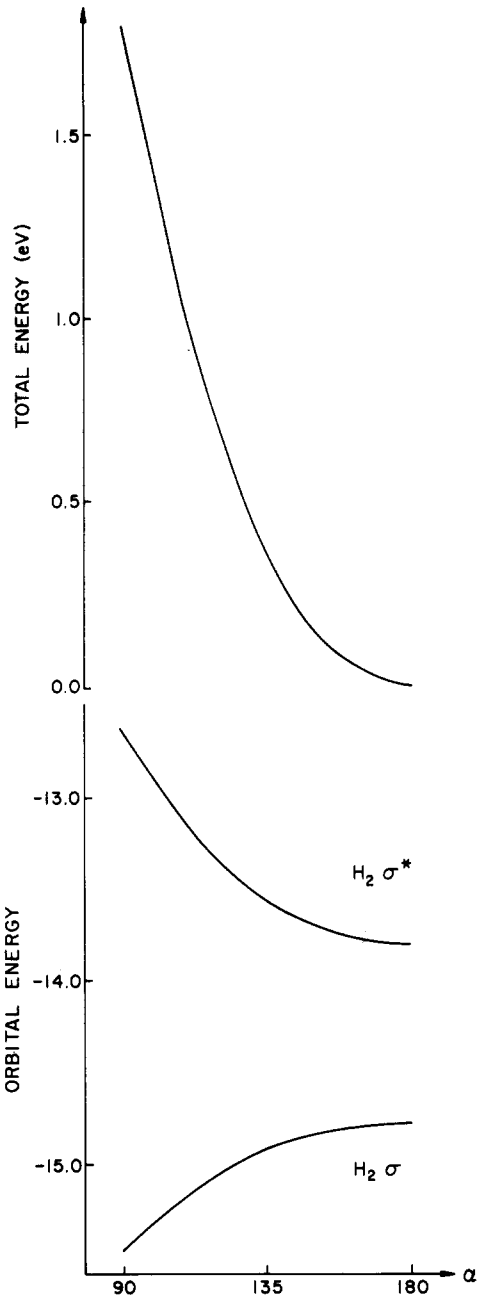

Figure 5.

Cp_2Sm^+ orbitals of b_2 symmetry. Delocalization into the $SmCp_2^+$ orbitals stabilizes both the H_2 σ and σ^* orbitals. As α is varied, the two hydrides approach each other; the net effect is repulsive. Stabilization of the H_2 σ orbital is exceeded by destabilization of the H_2 σ^* orbital. Computed overlap populations between the hydrogen atoms indeed become more negative as α decreases.

A decrease in α also deprives the H_B orbital of overlap with the b_2 orbitals of the Cp_2Sm^+ fragments. Both of these effects could also be observed for an analogous distortion of diborane. The present system is distinct in that the Cp_2Sm^+ fragment, unlike BH_2, has a low-lying empty b_1 level. The loss of H_B–$1b_2(Cp_2Sm)$ overlap population is balanced by the increase in H_B–$1b_1$ overlap population. The overall loss of H_B–Cp_2Sm overlap population may be traced to a decline in H_B–$1a_1$ overlap (see Figure 6). At $\alpha = 180°$, the H_B orbital overlaps with the central lobe of the x^2 orbital, a principal constituent of the Cp_2Sm $1a_1$ fragment molecular orbital. As α is reduced, the H_B orbital approaches the node of the x^2 orbital (see **20**). The H_B orbital originally interacts with the circular projection of the x^2 orbital in the yz plane. At $\alpha = 90°$, H_B is in the xz plane and realizes much less overlap with x^2. Interactions with the $2a_1$ orbital, which has large $z^2 - y^2$

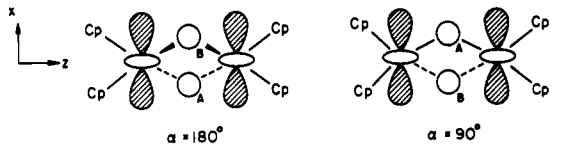

20

contributions, run counter to the $1a_1$ interactions, although the magnitudes of the overlap populations are not as large. H_B initially lies close to the node of the $z^2 - y^2$ orbital. At $\alpha = 90°$, the H_B orbital sees only the lobe along the z axis.

In the previous distortion, the H_2 σ^* destabilization and the overlap effects between H_B and the Cp_2Sm fragment orbitals favored the $\alpha = 180°$ structure. Should the stationary H_A atom be fixed in the Sm_2Cp_4(centroid) plane, however, as in **21**, with

21

β the free dihedral angle, these two factors will work against each other. H_2 σ^* destabilization favors $\beta = 180°$. Hydride to Cp_2Sm bonding favors $\beta = 90°$. A compromise is computed to be reached at $\beta = 135°$. As in the previous case, the $1b_1$ and $1b_2$ interactions with H_B move in opposite directions with the dihedral angle changes and approximately cancel each other's effect on the energy.

Now let us effect a twisting of dihedral angles without changing the distance between the hydrides. One way to do this is to keep the Sm_2H_2 plane of the symmetrical structure but to vary its dihedral angle with the Sm_2Cp_4(centroid) plane (**22**). As γ

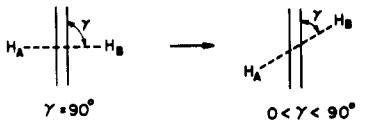

22

decreases, the energy rises (Figure 7) for the reasons that might have been surmised on the basis of the last two distortions. Overlap population with $1a_1$ of the $SmCp_2$ group declines with γ, but this trend is partially offset by the $2a_1$ interaction. The rise of H–$1b_1$ bonding balances the fall for H–$1b_2$.

In all the calculations of distortions, the Cp(centroid)–Sm–Cp(centroid) angle has been frozen at 130°. Variation of this angle will have some minor effects on the Cp_2Sm–H interactions. As the angle is compressed, $1a_1$ will acquire more z^2 character and will start to forsake its x^2 origin. p_z contributions also increase as the angle is reduced. Therefore, the preference of the $1a_1$ orbital for hydride in the plane perpendicular to Cp(centroid)–Sm–Cp(centroid) over hydride in the plane parallel will be reduced. To a z^2 orbital mixed with p_z, such geometrical variations should not matter much. Similarly, as $2a_1$ goes from being like $z^2 - y^2$ to geometries where $x^2 - y^2$ is a better description, the distinction between hydrides in the xz vs. yz planes should disappear.

Another geometrical variation that will be of interest later in this discussion is shown in **23**–**25**. At all times the dihedral angle

23 24 25

between the two Sm_2H planes is 90°. The ordering of the energies is **23** < **24** < **25**; no barriers to interconversion were discovered

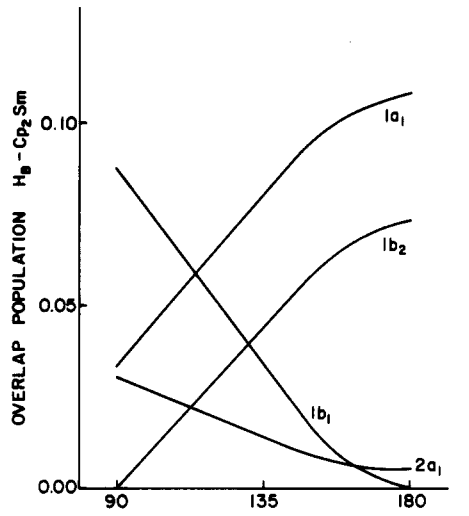

Figure 6.

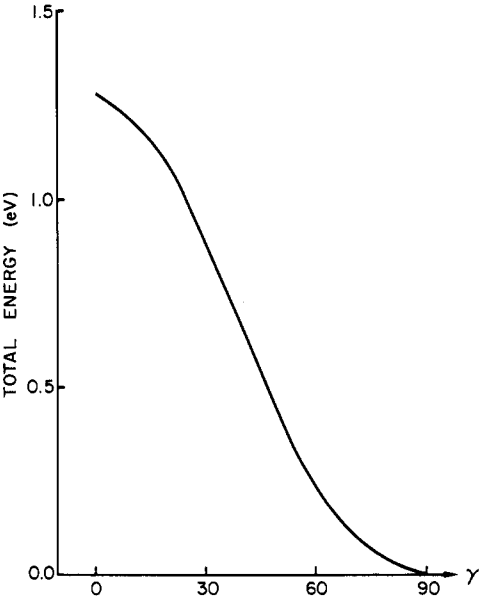

Figure 7.

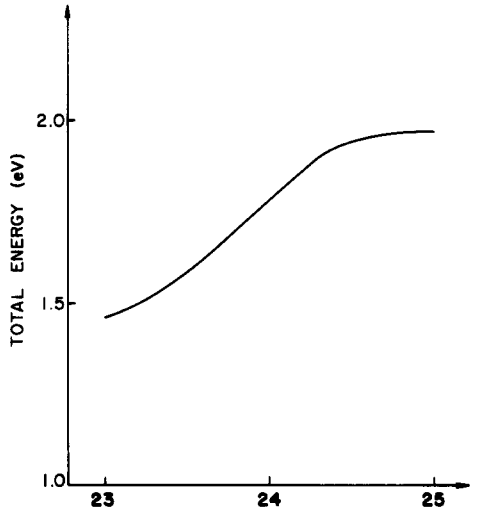

Figure 8.

(Figure 8). As might have been expected, the structure that most resembles the reference structure is favored. The dropoff of the H–Cp_2Sm bonding overall is sharpest when the Sm_2H dihedral angle with the Cp(centroid)–Sm–Cp(centroid) plane approaches 0°.

Cp_2Ln Tri- and Tetrahydrates

How might an additional hydride attach itself to the reference $(Cp_2SmH)_2$ complex? The negligible participation of the $2a_1$ and $1b_1$ fragment MO's of Cp_2Sm^+ in the binding of the two bridging hydrides suggests that two types of acceptor sites are available. The $2a_1$ Cp_2Sm orbital, primarily a $z^2 - y^2$ orbital, has a lobe pointing in the y direction. Calculations on $(Cp_2SmH)_2H^-$ place the extra hydride in the Sm_2H_2 bridge (yz) plane, as in **26**.

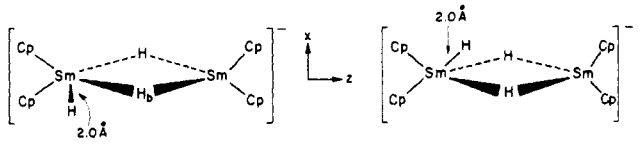

26 **27**

Overlap populations with the $1a_1$ and $1b_1$ orbitals of the nearby Cp_2Sm^+ fragment are 0.05 and 0.01, respectively, but the chief source of the 0.42-eV binding energy relative to $H^- + (Cp_2SmH)_2$ is the extra hydride's overlap population with the $2a_1$ orbital of 0.13. The terminal hydride to Sm bond length of 2.0 Å is taken from a similar Zr complex's structure;[3] the terminal hydride to Sm bond is parallel to the y axis. This extra hydride resists motion that alters the H_t–Sm–H_b angle of approximately 60°. Motions out of the yz plane result in rapid loss of overlap population with the $2a_1$ Cp_2Sm orbital. Repulsions with other ligands about the Sm, especially the bridging hydrides, and overlap with the Cp_2Sm $2a_1$ orbital determine the terminal hydride's position.

As was mentioned before, motion of the terminal hydride out of the yz plane produces a rise in energy due to loss of overlap with the $2a_1$ Cp_2Sm orbital. On the basis of the hope that the $1b_1$ Cp_2Sm orbital might come to the rescue, geometries of the type **27** were investigated. Unfortunately, with the Cp(centroid)–Sm–Cp(centroid) angle set to 130°, the terminal hydrogen atom comes uncomfortably close to the atoms of the Cp ring. Terminal hydrides that donate electron density to the $1b_1$ Cp_2Sm orbital are not feasible.

If the Sm–H_t bond length is increased to 2.29 Å, the Sm–H_b length obtained from previous calculations, more promising hypothetical structures result. With the hydride restricted to the Sm_2Cp_4 (xz) plane, a structure (**28**) with the angle between the

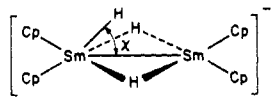

28

Sm–H and Sm–Sm vectors, χ, equal to about 45° was obtained. This suggested the placement of the extra hydride in a bridge position, equidistant from the two Sm atoms. The deployment of the hydrides is symbolized by **29**. The total energy of this

29 **30**

structure is 1.9 eV above the $(Cp_2SmH)_2 + H^-$ limit, due chiefly to the H_A–H_C distance of 1.70 Å. Noteworthy in this calculation is the $1b_1$ Cp_2Sm to H_C overlap population of 0.11. Overall, the interaction of the H_C hydride orbital with the symmetric combination of H_A and H_B (mixed with $1a_1$ orbitals of the Cp_2Sm fragments) is repulsive.

Suppose that this antagonism is alleviated somewhat by arranging the hydrides as in **30**. The energy declines by 1.3 eV. The H_A–H_B overlap population climbs from −0.07 to −0.03; the $1a_1$ to H_C overlap population rises from −0.46 to 0.03. Repulsions between hydrides have been reduced. The $1b_1$ Cp_2Sm overlap population with H_C goes from 0.12 to 0.11, an insignificant decline.

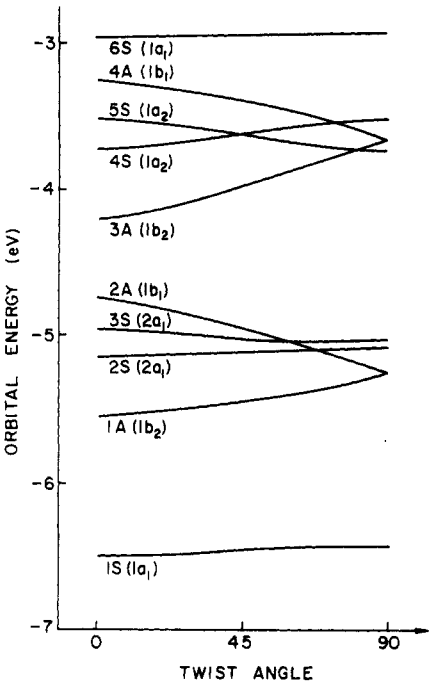

Figure 9.

In summary, the placement of additional electron-pair donors on the symmetric $(Cp_2SmH)_2$ complex may take advantage of two empty d-like orbitals on the Cp_2Sm fragments. Terminal ligands in the Sm_2H_2 plane donate to the $2a_1$ orbital of Cp_2Sm, and bridging ligands in the Sm_2Cp_4 plane donate to the $1b_1$ orbitals of the Cp_2Sm fragment. In the latter case, a symmetric combination of the $1b_1$ orbitals is available, so that one could imagine the addition of two hydrides to give a tetrabridged structure (**31**).

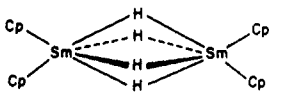

31

Twisting the Cp_2Sm Planes Relative to Each Other

The previous calculations have maintained the coplanarity of the two Cp(centroid))$_2$Sm planes. Let us now consider twisting one of the Cp(centroid)–Sm–Cp(centroid) planes so that the dihedral angle of this plane with its partner on the other Sm center becomes 90°, as indicated symbolically in **32**. Suppose further

32

that the bridging hydrides are eliminated from the molecule, but with the remaining internuclear distances of $(Cp_2Sm)_2^{2+}$ remaining intact. The twisting of the dihedral angle reduces repulsions between Cp rings. With a dihedral angle of 90°, the energy is about 0.8 kcal/mol (about 0.03 eV) lower than that of the original eclipsed structure.

Effects of changing this dihedral angle on the d-orbital levels of $(Cp_2Sm)_2^{2+}$ are summarized in the Walsh diagram of Figure 9. All of these energy levels are unoccupied, so their behavior has no effect on the total energy. The lowest level depicted in the diagram is a bonding combination of the two Cp_2Sm^+ $1a_1$ fragment MO's, the x^2-like orbitals. Its energy rises slightly as the x axis of the one of the Cp_2Sm^+ fragments forms a 90° angle with the x axis of the other Cp_2Sm^+ fragment. The overlap integral steadily declines from 0.51 to 0.49.

The symmetry operation that is preserved throughout the variation of dihedral angle is the C_2 axis defined by the two Sm

atoms. The lowest levels classified as antisymmetric with respect to this operation are formed from the b_1 and b_2 fragment MO's of the Cp_2Sm^+ fragments. When the dihedral angle reaches 90°, the levels become degenerate bonding combinations. A similar trend obtains for the antibonding combinations, 3A and 4A. Bonding and antibonding combinations of the Cp_2Sm^+ $2a_1$ fragment MO's (2S and 3S) have a small splitting due to an overlap integral that never exceeds 0.06. To the extent that donation to the 1S and 1A levels occurs, the preference for the twisted structure will be offset.

The degeneracy of the 1A and 2A levels at a 90° dihedral angle implies the existence of four equivalent bridging sites between the Sm atoms. The first two hydrides (or other σ electron pair donors) can be expected to occupy positions between the Sm atoms. Since the 2A level ends up below the 2S and 3S levels, extra hydrides may occupy the remaining bridging positions instead of the terminal positions. Splittings of the 1A, 2A, 2S, and 3S levels are smaller when the dihedral angle is 90°; fluxional behavior with respect to the hydride positions may obtain.

Suppose that the twisting of one of the Cp–Sm–Cp planes is repeated in the presence of the bridging hydrides. To represent this process, the dihedral angle δ (**33**) is varied, where the solid

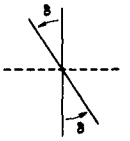

33

lines stand for Cp–Sm–Cp planes and the dotted line stands for the Sm_2H_2 plane. Going from $\delta = 0°$, the reference structure, to $\delta = 90°$ costs 0.6 eV. One can account for this rise with the orbitals of the $(Cp_2Sm)_2^{2+}$ fragment, but we will not go through the argument here. With the dihedral angle between the Cp–Sm–Cp planes fixed at 90°, we can return to the question of the hydride positions. Hydrides equidistant from the Sm atoms form Sm–H–Sm planes. The variation of the dihedral angle of one such Sm–H–Sm plane with the Cp–Sm–Cp planes is represented by **34**. The position of H_A is fixed such that the Sm–H_A–Sm plane

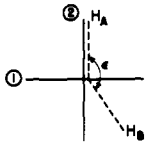

34

has dihedral angles with the first and second Cp–Sm–Cp planes of 90 and 0°, respectively. The Sm–H_B–Sm plane forms a dihedral angle of ϵ with the Sm–H_A–Sm plane.

$\epsilon = 180°$ gives the lowest energy, which is below that of the $\epsilon = 90°$ structure by 1.2 eV. This result is similar to what occurs for **35**, a case we discussed earlier, where the energy difference

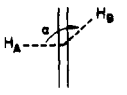

35

between the two corresponding structures is 1.8 eV. In the latter case, the $H_A^-H_B^-$ repulsions are compounded by the preference of the Cp_2Sm groups in the plane perpendicular to the Cp–Sm–Cp plane. When one of the Cp–Sm–Cp planes is twisted 90°, there are four more or less equivalent bridging positions. Therefore, as α goes from 180 to 90°, losses in overlap population between H_B and the first Cp_2Sm fragment are partially compensated by gains in overlap population with the second Cp_2Sm fragment. This leaves the repulsions between hydrides as the major obstacle to decreasing α.

The structures represented by **36** are lower in energy than their

36

counterparts **37**, but higher in energy than **35**. A simple for-

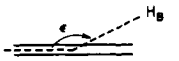

37

mulation of this ordering is that the hydrides prefer to be in Sm–H–Sm planes that are perpendicular to Cp–Sm–Cp planes. This trend holds for $90° < \epsilon < 180°$, but for $\epsilon = 90°$ the energies are approximately the same.

As usual, the main participants in bonding to the hydride bridges are $1a_1$, $1b_1$, and $1b_2$ fragment MO's of the Cp_2Sm units. When α is varied from 180 to 90°, the first Cp_2Sm $1b_2$ overlap population with H_B (see **34**) goes from 0 to 0.087 and its partner fragment MO, $1b_1$, goes from 0.077 to 0. Similarly, for the second Cp_2Sm $1b_2$ to H_B overlap population, the variation is from 0.082 to 0, while the $1b_1$ overlap population goes from 0 to 0.081. In other words, the sums of all the Cp_2Sm $1b_1$ and $1b_2$ fragment MO interactions with the hydrides remain nearly constant. The big changes occur in the Cp_2Sm $1a_1$ interactions with the hydrides. The second Cp_2Sm $1a_1$ overlap population goes from 0.11 to 0.02 from $\alpha = 180°$ to $\alpha = 90°$, and the first Cp_2Sm $1a_1$ overlap population goes from 0.07 to 0.11. The x^2 character of this orbital suffices to explain the preference for $\alpha = 180°$ and the energy ordering of the three structures (**38**).

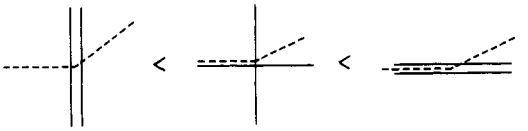

38

In a geometrical transit that freezes the distance between hydrides, the preferences of the fragment MO's are more ambiguous. Again, with the dihedral angle between the two Cp–Sm–Cp planes fixed at 90°, the Sm_2H_2 quartet of atoms is locked in a plane. The dihedral angle of this plane with the Cp_4Sm_2 frame, ω (**39**),

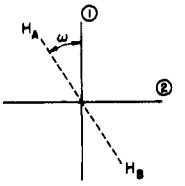

39

is varied. The $\omega = 45°$ configuration is actually preferred to $\omega = 0°$ by about 0.09 eV. No overriding trends involving overlap populations or orbital energies emanate from these calculations. It suffices to say that, depending on the detailed balancing of electronic and steric factors, different values of ω may be observed.

The equanimity of the Sm_2Cp_4 framework toward Sm_2H_2 plane rotations is continued when the Sm_2H_A planes have a dihedral angle of 90°, as in **40**. This geometrical variation favors $\eta = 45°$

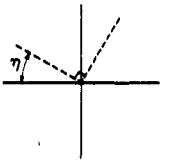

40

over $\eta = 0°$ by 0.09 eV. As in the previous case, there are no

dominant trends that reflect a steadfast principle of bonding. One may expect that the structures with the 90° dihedral angle between the Sm_2H_A and Sm_2H_B planes will be unfavorable relative to those where the hydrides are more remote from each other. The energy difference between **41** and **42** is generally about 0.17 eV.

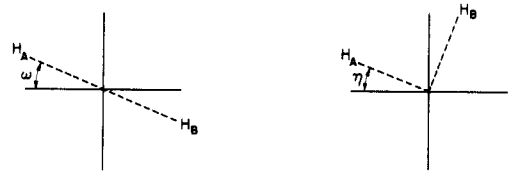

41 **42**

Similar arrangements of the bridging hydrides are expected when each Sm has a terminal hydride also. The terminal hydride demands the attention of the $2a_1$ MO of each Cp_2Sm fragment. The action of the $1a_1$, $1b_1$, and $1b_2$ orbitals on bridging hydrides is undisturbed. At the same time, the repulsions between bridging and terminal hydrides will play a role in determining the geometry. For example, if the two Cp_2Sm planes are parallel, one expects the terminal hydrides to reside in a perpendicular plane. On the basis of the previous calculations, the bridging hydrides will lie in the same plane. A series of calculations in which the plane containing the bridging hydrides and the Sm atoms is allowed to rotate (**43**) produces a nonzero angle between the $Sm_2(H_b)_2$ plane

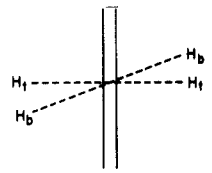

43

and the $Sm_2(H_t)_2$ plane. Repulsions between the bridging and terminal hydrides do play a part for these structures. In case the two Cp_2Sm planes are orthogonal, there are two structures that give a 45° dihedral angle for the $Sm_2(H_b)_2$ plane. These differ in energy by a miniscule amount. A barrier to rotation of the plane between the two stable forms (**44**) amounts to 0.18 eV, the maximum energy occurring when the $Sm_2(H_b)_2$ plane eclipses one of the Cp_2Sm planes.

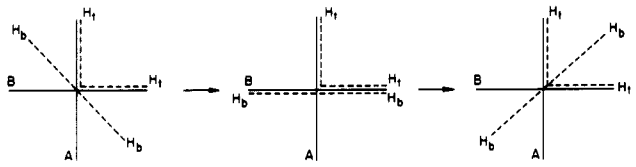

44

Moving across the Lanthanide Series

Experimentally one can usually produce a variety of organolanthanide species, so that it becomes interesting to outline the differences, if any, as one changes the element. There should be some variation in the diagonal matrix elements of the Hamiltonian, the H_{ii}'s. These energies are taken to be averages of the spin–orbital energies from Desclaux's relativistic atomic calculations.[8] Some of these numbers are given in Table I. The 6p and 7p parameters are chosen to be the same as the 6s and 7s parameters, respectively. f-orbital levels are ignored here, since in all applications undertaken for lanthanides so far, no chemical importance is attached to these orbitals. In the sixth period, one notices no great differences between La, Ce, and Hf. In going across the inner transition file, however, the 6s and 5d levels cross each other. H_{ss} is lower than H_{dd} in period 7 as well, except for Th.

The spatial extent of the atomic orbitals changes little within the lanthanide series, so a comparison between $SmCp_2$ and $LuCp_2$

(8) Desclaux, J. P. *At. Data Nucl. Data Tables* **1973**, *12*, 317–59.

Table I. H_{ii} Parameters (eV) for Inner Transition Elements

	La	Ce	Gd	Lu	Hf
6s	−4.89	−4.97	−5.44	−6.05	−4.84
5d	−6.41	−6.43	−6.06	−5.22	−6.56

	Ac	Th	Pa	U	Np	Lw	104
7s	−5.19	−5.70	−5.41	−5.51	−5.60	−6.74	−6.75
6d	−4.79	−5.90	−5.08	−5.12	−5.11	−4.11	−4.11

Table II. Metal Atomic Orbital Contributions for MCp_2 MO's

symmetry	energy, eV	electrons in AO's
		Lutetium
$1a_2$	−2.51	1.80 xz
$1b_1$	−3.37	1.67 xy, 0.19 x
$2a_1$	−4.34	0.62 z^2, 0.95 x^2-y^2, 0.06 z, 0.05 s
$1b_2$	−4.67	1.07 yz, 0.62 y
$1a_1$	−5.59	0.69 z, 0.68 s, 0.33 z^2, 0.29 x^2-y^2
		Samarium
$1a_2$	−3.63	1.90 xz
$1b_1$	−4.19	1.9 xy
$2a_1$	−5.02	0.70 x^2-y^2, 0.67 z^2, 0.05 z, 0.01 s
$1b_2$	−5.02	1.9 yz
$1a_1$	−5.29	0.62 x^2-y^2, 0.51 z^2, 0.48 s, 0.36 z

will tell us something about the chemical effects of the H_{ii} choices. With the Cp–M–Cp angle fixed at 130°, orbitals summarized in Table II result. H_{dd} being higher than H_{ss} and H_{pp} causes two main changes. $1a_1$ is no longer x^2-like: its s and p_z character contribute to a lobe that points away from the Cp rings. $2a_1$ of $LuCp_2^+$ is more like a x^2-y^2 orbital and less like a y^2-z^2 orbital. Both fragments have b_2 orbitals available for bonding.

In previous sections, we saw how the fragment MO's of $SmCp_2^+$ bond with bridging hydrides as the hydride is twisted out of the yz plane and into the xz plane. The preferences of the b_1 and b_2 orbitals generally canceled each other out. Nodal properties of the x^2-like orbital, $1a_1$, proved decisive in explaining the reluctance of the hydrides to undergo such distortions. With the increased contributions of s and p_z in the $1a_1$ orbital of $LuCp_2^+$, this trend may not be as important in determining the positions of bridging hydrides. Thus, the effect of changing the Cp–M–Cp angle may be reinforced or moderated by changes in the metal's atomic orbital energy levels.

Model for the $Cp_6Er_3H_3Cl^-$ Trimer Hydride

The molecule in question, an interesting lanthanide cluster hydride, is just a little too big for our computer programs. So we replaced Cp^- by three hydride anions, i.e. studied LaH_6^{3-} in place of $LaCp_2^+$. We also used the lutetium parameters as a better approximation to erbium than samarium, so that the calculation was on LuH_6^{3-}. Two equilateral triangles of hydrides (residing where the localized π orbitals of the Cp ring would be) are employed. Once again, the angle described by the centroid of one triangle, the metal atom, and the other centroid is 130°. Orbital energies are slightly lower than for $LuCp_2^+$ (by between 0.2 and 1.0 eV), but the percentages of metal atomic orbital character are nearly the same.

Plots of the LuH_6^{3-} orbitals are shown in Figure 10. The yz plane, normal to the H_3(centroid)–Sm–H_3(centroid) plane, is depicted. The $1a_1$ orbital is similar to the $2a_1$ orbital of the $TiCp_2^{2+}$ fragment.[6] This orbital has one lobe pointing away from the ligands with a slight dimple on the side near the ligands. The $1b_2$ orbital is a combination of yz and p_y directed away from the ligands. Finally, the $2a_1$ ligand's largest lobes lie along the y axis, with z^2 combinations giving the central lobe the opposite sign.

When the LuH_6^{3-} units are arranged in an equilateral triangle of sides 3.7 Å (between the Lu atoms),[5] the unoccupied d levels mix according to the scheme of Figure 11. The $1a_1'$ level is a symmetric combination of the LuH_6^{3-} $1a_1$ levels and should be ideally suited for stabilizing an s orbital in the center of the triangle. Degenerate combinations of the $1b_2$ orbitals of LuH_6^{3-} are next, shown in **45**. Next is the symmetric combination of LuH_6^{3-} $2a_1$ levels, the $2a_1'$ orbital of the trimer (**46**). These are

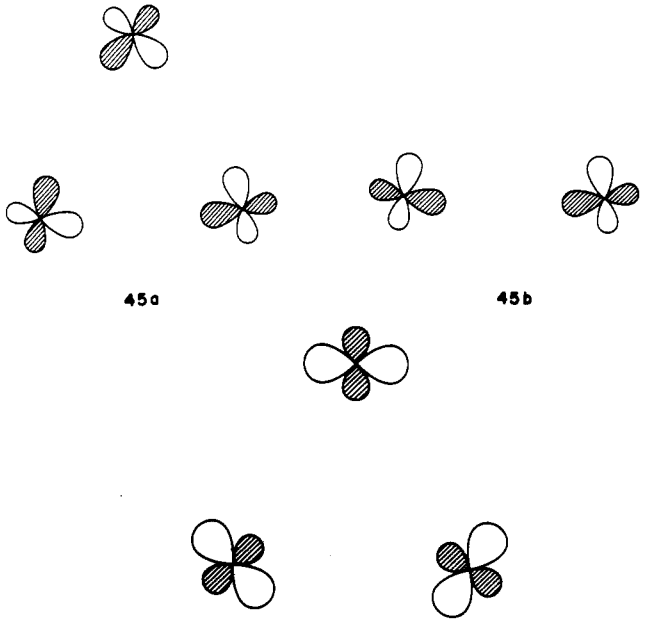

45a 45b

46

the main actors in the interaction with the bridging hydride and chloride. Three such bridging groups, e.g. hydrides, would also give e and a_1 combinations **47** and **48**. These are a nice match

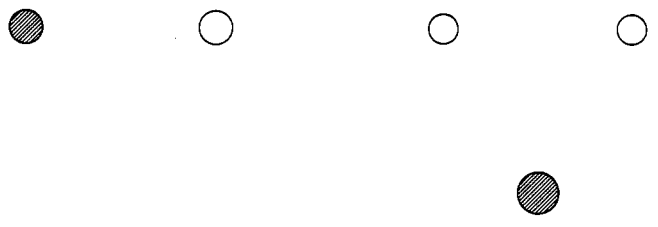

47

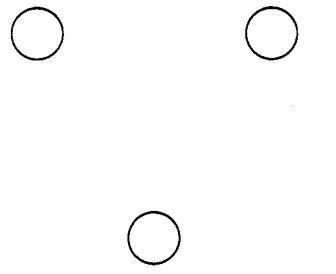

48

for **45** and **46**, respectively.

Calculations on $(LuH_6)_3H_4^{13-}$ corroborate this reasoning. The bridging hydrides are 2.4 Å from both the nearest Lu atoms. Dividing this molecule into three fragments, $(LuH_6)_3^{9-}$, H_3^{3-}, and H^-, allows overlap populations between the fragment MO's to be calculated. The central hydride orbital has an overlap population of 0.52 with $1a_1'$ of $(LuH_6)_3^{9-}$, but only 0.11 with $2a_1'$. On the other hand, the $1a_1'$ orbital of H_3^{3-} has an overlap population of 0.32 with $2a_1'$ of $(LuH_6)_3^{9-}$ and only 0.12 with $1a_1'$. The mixing of the H_3^{3-} and $(LuH_6)_3^{9-}$ e sets gives overlap populations of 0.50 for each interaction. All other bonding interactions are negligible by comparison.

Now let us go from hydride bridges to chloride bridges. The Lu–Lu distance is increased to 3.9 Å and the Lu to bridging Cl^- distance is 2.7 Å. In D_{3h} symmetry, the central chloride's s and p_z orbitals will transform according to the a_1' and a_2'' irreducible representations, respectively, while the p_x and p_y orbitals form a set of e' orbitals. The three bridging chlorides have s orbitals that form a_1' and e' combinations. p_z orbitals of these atoms become a_2'' and e'' after symmetry projection. One can rotate the p_x and p_y orbitals on each chloride so that one p orbital points toward the centroid of the Cl_3^{3-} triangle and the other p orbital is perpendicular to the line connecting the chloride to the centroid (**49**). Calling the former group the p_c orbitals and the latter the p_p orbitals, one easily sees the p_c orbitals forming a_1' and e' orbitals and the p_p orbitals forming a_2' and e' combinations.

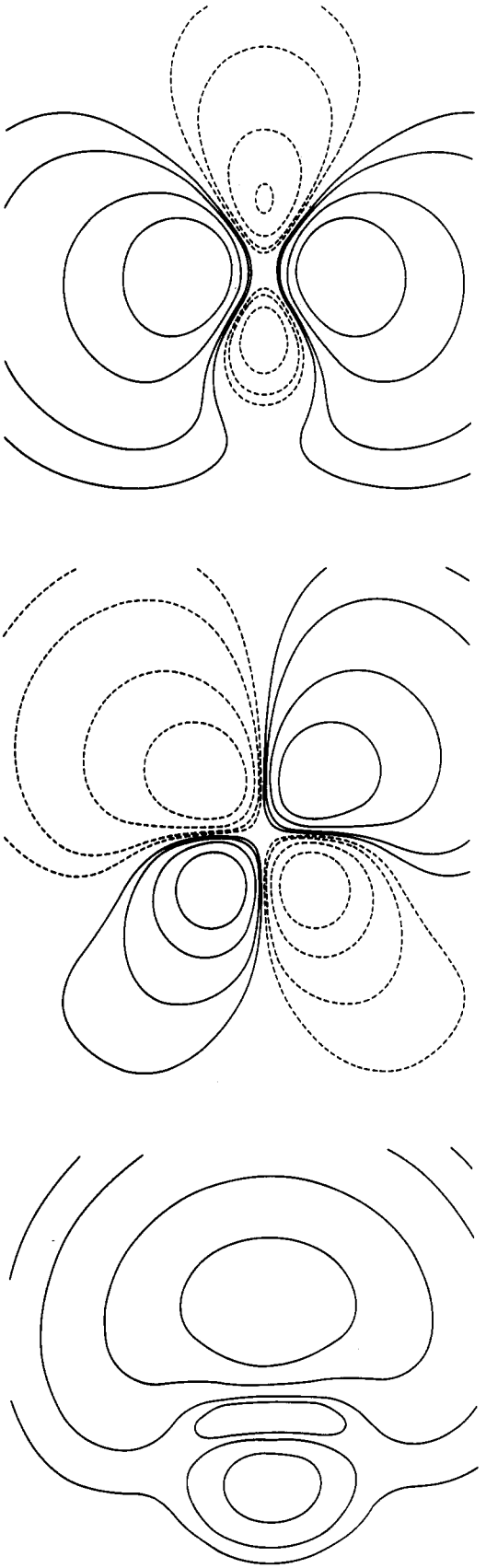

Figure 10. LuH_6^{3-} orbital plots: (bottom) $1a_1$; (center) $1b_2$; (top) $2a_1$. All plots are in the *yz* plane.

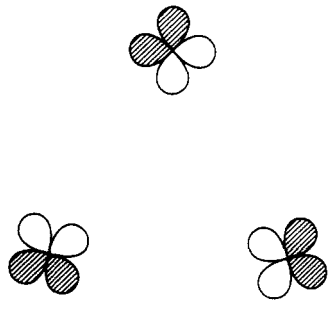

49

An examination of the final overlap populations between the Cl^-, Cl_3^{3-}, and $(LuH_6)_3^{9-}$ fragments shows which interactions are most important. By far the biggest interaction is between the s orbital of the central chloride and the $1a_1'$ orbital of $(LuH_6)_3^{9-}$. This overlap population of 0.41 is benefited partly by its closer Lu–Cl distance of 2.25 Å. Next in importance is the 0.29 overlap population obtained for the e′ combination of the Cl_3^{3-} s orbitals interacting with the 1e′ orbital of $(LuH_6)_3^{9-}$. $2a_1'$ and $1a_2''$ of $(LuH_6)_3^{9-}$ stabilize the a_1' combination of the bridging chlorides' s orbitals and the p_z orbital of the central chloride, respectively. These overlap populations are about 0.24. A surprisingly large overlap population of 0.25 occurs between the a_2' combination of the p_p orbitals and the very high lying a_2' combination of the LuH_6^{3-} $1b_1$ orbitals (**50**).

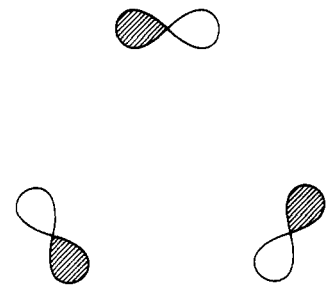

50

A crystal structure report on the anion $(ErCp_2)_3H_3Cl^-$ shows little symmetry.[5] For the purpose of calculations, the C_{2v} model **51** is used. The chloride, central hydride, and top Lu atom define

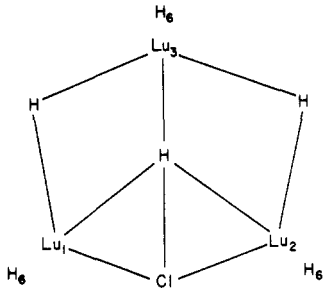

51

the C_2 axis. In the experimental structure, only the Lu–Lu distance seem to retain this symmetry. All of the other distances, especially those involving hydrides, are different from each other. Many calculations were done in an effort to expose the source of these apparent asymmetries. Unfortunately, none were discovered; the calculations support the C_{2v} hypothesis. The energy was lowered when the central hydride was slightly closer to the Lu_3 atom than to the Lu_1 and Lu_2 atoms. The external hydrides could be moved closer to Lu_3 without an energetic penalty. In fact, this probably is another instance of the calculations producing unreliable bond lengths. A similar effect obtained when these same hydrides were moved close to Lu_1 and Lu_2. What is interesting, however, is the energy maximum that emerged when the bridging hydrides were placed on normals from the midpoints of the Lu_1–Lu_3 and Lu_2–Lu_3 bonds. These hydrides will sit on one side or the other, but not in the middle.

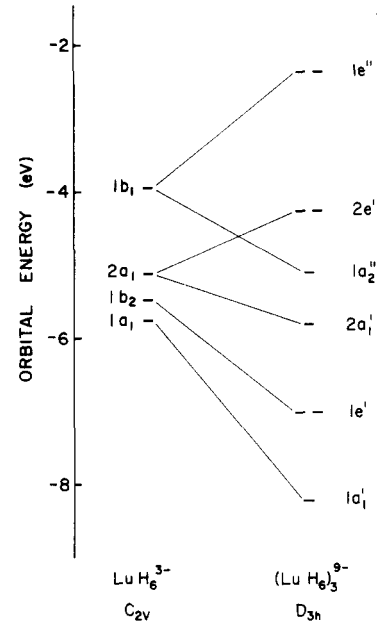

Figure 11.

Table III. Parameters Used in Extended Hückel Calculations[a]

orbital		H_{ii}, eV	ζ_1	ζ_2	coeff 1	coeff 2
Sm	6s	−4.86	1.400			
	6p	−4.86	1.400			
	5d	−6.06	2.747	1.267	0.7184	0.4447
	4f	−11.28	6.907	2.639	0.7354	0.4597
Lu	6s	−6.05	1.666			
	6p	−6.05	1.666			
	5d	−5.12	2.813	1.210	0.7044	0.4880
	4f	−22.40	9.136	3.666	0.7330	0.4459
C	2s	−21.40	1.625			
	2p	−11.40	2.275			
H	1s	−13.60	1.300			

[a] The d and f orbitals are formed by a linear combination of two simple Slater functions.

Acknowledgment. We are grateful to the National Science Foundation for its support of this work through Research Grant CHE 7828048 to Cornell University. Acknowledgment is made (by J.V.O.) to the donors of the Petroleum Research Fund, administered by the American Chemical Society, and to the Sandia University Research Program for partial support of this research. Discussions with W. J. Evans were important to us in stimulating this work.

Appendix

All calculations were performed by using the extended Hückel method[9] with weighted H_{ij}'s.[10] The extended Hückel parameters used in our calculations are listed in Table III. Parameters for Lu and Sm were obtained from the spin–orbital energies and expectation values of ref 8. An average over the spin components for each orbital energy was used to estimate the H_{ii} parameters. A similar average was taken for the value of r at which the orbital amplitude is a maximum, the expectation value of r, and the expectation value of r^2. All three of these values were used to choose the exponents and coefficients of the d and f orbitals; only the r expectation values figured in the ζ values for s and p orbitals. Parameters for the 5d orbital of Sm were obtained by interpolation between the d orbitals of Ce and Gd.

(9) Hoffmann, R. *J. Chem. Phys.* **1963**, *39*, 1397–1412. Hoffmann, R.; Lipscomb, W. N. *J. Chem. Phys.* **1962**, *36*, 2179–89. Hoffmann, R.; Lipscomb, W. N. *J. Chem. Phys.* **1962**, *37*, 2872–83.
(10) Ammeter, J. H.; Bürgi, H.-B.; Thibeault, J. C.; Hoffmann, R. *J. Am. Chem. Soc.* **1978**, *100*, 3686–92.